SSC22-VIII-07

Low-Thrust Reconfiguration Strategy for Flexible Satellite Constellations

Federica Paganelli Azza, Pietro De Marchi, Matteo Stoisa, Paolo Gennaro Madonia
AIKO S.r.l.
Via Dei Mille 22, 10123, Torino, Italy; +393408154418
federica@aikospace.com

ABSTRACT

Flexible and responsive space systems are needed to satisfy changing mission requirements and react to unforeseen challenges. Reconfigurable constellations are a promising approach to overcome limitations of the current design philosophy, offering operators the ability to actively adapt the constellation configuration to future needs, promptly modifying their pattern to focus the available resources towards dynamic objectives. This work introduces a low-thrust reconfiguration strategy to optimize these constellations through a multi-objective Genetic Algorithm able to trade-off between observation performance over a desired target area and maneuvering cost to reach the new pattern. The presented approach is validated in a LEO scenario, considering the reconfiguration from a global coverage to a regional one. The obtained results are compared with the ones available in literature to show the suitability of the proposed solution.

INTRODUCTION

Constellations of satellites working collectively towards a common purpose are traditionally used to achieve global coverage for both Earth observation or telecommunication applications. Currently adopted architectures are mostly constituted by fixed orbits in which satellites occupy a predetermined position throughout their whole operational life. This mission design philosophy is well suited for non-maneuverable satellites that are not allowed to move away from their slot once that they have been deployed. However, recent advances in electric propulsion technologies for small satellites are enabling disruptive capabilities, offering new opportunities in the design and operation of satellite constellations. In particular, the possibility of reconfiguring the constellation geometry once the mission is already in its operational phases is becoming increasingly appealing to focus the available resources towards changing objectives. A wide spectrum of EO missions highly benefits from flexible configurations in which the constellation orbits could be re-optimized in order to satisfy new observation requirements and access specific targets more quickly. This allows, for instance, to reconfigure the constellation when one or more satellites have failed[1] or to integrate new satellites into an existing system.[2] Furthermore, being able to adapt the satellites' geometry in response to changes in the region of interest to be covered plays a fundamental role in several applications, such as disaster monitoring, reconnaissance and atmospheric research.[3,4] Reconfigurable constellations may also be relevant in Satellite-as-a-Service scenarios, allowing the usage of a single platform or a reduced set of them to satisfy the needs of stakeholders interested indifferent kinds of services.

Reconfiguration has not been implemented yet in any space mission but it has recently been investigated by several research groups, such as deWeck's,[3,5,6] Mortari's[7] and Ferringer's.[8] In particular, the concept of reconfigurable satellite constellation (ReCon) has been proposed[9] as a design strategy to enable a two-mode observation constellation that switches from a Global Observation Mode (GOM) to a Regional Observation Mode (ROM) for contingent responses.

Our research work investigates reconfigurable constellations opportunities and focuses on the development of a flexible low-thrust reconfiguration strategy aimed to provide feasible geometries that guarantee enhanced coverage over a desired target. The reconfiguration problem is formulated as a multi-objective optimization in which a trade-off between observation performance over a given area of interest and cost to perform reconfiguration maneuvers should be produced. Constraints on the available resources are taken into account during the optimization so as to provide only target constellations that could be reached from the initial configuration.

The paper is organized as follows. The second section presents the mathematical models adopted to describe the problem. The third section details the constellation reconfiguration problem and its multi-objective optimization using a Genetic Algorithm. Simulation results for a LEO constellation

are given in the following section. Final remarks and future work are illustrated in the last section.

MATHEMATICAL MODELING

Constellation Model

Each orbit in the target constellation is specified in terms of keplerian parameters by specifying its semi-major axis a, eccentricity e, inclination i, right ascension of the ascending node Ω, argument of the perigee ω and true anomaly ν. The satellite coverage is modeled assuming a circular Field Of View (FOV) and the swath length l_s is computed according to the spherical-Earth approximation[10] as:

$$l_s = R_E \tan \lambda \tag{1}$$

where R_E is the Earth radius and λ is the Earth central angle.

The propagation of satellites' position and velocity is performed with a numerical Runge-Kutta-Fehlberg (RKF45) variable step integrator available in Basilisk Astrodynamics simulation framework.[11] The GGM03S gravitational field[12] is adopted and spherical harmonics up to the 70^{th} degree[13] are included. In order to increase computational performance during the propagation phase, a multi-processing architecture[14] is exploited. The propagation of each satellite is performed within independent processes whose number is determined by the size of the constellation and the available hardware.

Starting from satellites' positions along the propagation horizon, the corresponding geodetic latitude and longitude can be computed as described in literature[15] to determine the observed Earth location at any time instant. In particular, visible sites are retrieved at each propagation step by looking at the target points inside the instantaneous FOV. This information is stored in a $N_i \times N_k$ matrix, where subscript i represents the target sites on the earth surface and k stands for the propagation time step, and used to compute area coverage and revisit time statistics, as presented in this subsection.

Target points are determined by dividing the Earth surface into several tiles of near-equal area.[16] In this way, sites are uniformly distributed all over the globe as shown in Figure 1. The size of each tile strictly depends on payload specifications and the parameters of the tessellation algorithm should be chosen to guarantee that at least one tile is fully within the FOV of each satellite in the constellation.

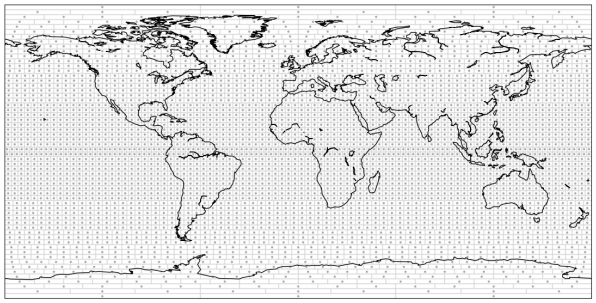

Figure 1: Target Sites Distribution for a FOV of 20 Degrees

Low-Thrust Maneuvers

Available literature on constellation reconfiguration has restricted the analysis to specific sets of maneuvers, such as in-plane maneuvers used to reach Repeating Ground Track (RGT) orbits[3] or to obtain the desired argument of latitude or RAAN separation between the satellites in the constellation.[17] However, since this work aims to analyze low-thrust reconfiguration opportunities and costs, the choice of predetermined available maneuvers or fixed final orbits is avoided and a general framework to evaluate the feasibility of a given maneuver should be developed.

The feasibility of transfers between an initial and target orbit is assessed in terms of required change in velocity ΔV. Since methods that rely on numerical simulation are too computationally expensive and cannot be executed for each candidate solution encountered during the optimization process, it is desirable to exploit a fast estimation of the ΔV. Analytical solutions for estimating the cost of low-thrust transfers in Low Earth Orbits are therefore employed and integrated in the optimization routine to produce only target orbits that could be reached from the initial configuration. In particular, two different maneuvering strategies are considered and the results obtained by inserting them in the optimization are presented and compared.

Separate Maneuvers Strategy

A first maneuvering strategy is defined following the approach proposed in literature[18] that starts from the Gauss form of the Lagrange Planetary Equations[19] and isolates the contributions to change specific orbital elements. In this way, analytical expressions to estimate the ΔV required to perform a change on a single orbital element can be retrieved.

The maneuvers needed to reach the target orbit are therefore assumed to be performed sepa-

rately on each orbital parameter by applying the optimal thrusting laws available in literature. Under this assumption, the overall ΔV cost can be retrieved directly from the expressions reported in literature.[18] An important remark is that changes in true anomaly are not considered amongst the contributions to the overall ΔV as desired in-plane phasing in the target orbit could be achieved through a proper time shift of the maneuvers. The requested target RAAN phasing is instead obtained by exploiting the natural drift produced by the Earth oblateness,[20] that is expressed as:

$$\dot{\Omega} = -\frac{3}{2}\sqrt{\frac{\mu}{a^3}} J_2 \left(\frac{R_E}{a}\right)^2 \frac{\cos(i)}{(1-e^2)^2} \tag{2}$$

where $\dot{\Omega}$ is the RAAN drift rate, μ is the standard gravitational parameter of the Earth, R_E is the Earth radius and J_2 is the Earth second degree geopotential contribution. The maneuver is performed in three phases: the semi-major axis is raised of an amount Δa to reach a coasting orbit, then, after a proper coasting duration, the orbit is decreased again to the initial height. The overall cost for the maneuver is therefore estimated as the ΔV requested for a semi-major axis change maneuver of $2\Delta a$. Numerical results reported in this section assume that a value of $100km$ is used as Δa.

An example of the described maneuvering strategy is given for a transfer where desired target values are imposed on semi-major axis, eccentricity and inclination. In particular, starting from a LEO orbit defined by the following set of keplerian parameters:

$$\begin{cases} a_0 = 6678km \\ e_0 = 0.01 \\ i_0 = 60\,\text{deg} \\ \Omega = 0\,\text{deg} \\ \omega = 0\,\text{deg} \\ \nu = 0\,\text{deg} \end{cases} \tag{3}$$

a target orbit with $a_t = 6978km, e_t = 0.04, i_t = 65\,\text{deg}$ has to be reached. Final values are not prescribed for RAAN, argument of the perigee and true anomaly, that are therefore left free to vary according to the chosen maneuver profile and external perturbations. The overall transfer is executed by means of three separate maneuvers, aimed at modifying separately a, e, i so as to approach the desired final orbit. In particular, a first maneuver is performed to increase the semi-major axis up to a_t, then the eccentricity is corrected and led to e_t and, finally, the inclination is changed to match i_t. The three maneuvers are simulated considering a CubeSat with initial mass equal to $15kg$ equipped with an Hall Effect Thruster with nominal thrust of $2.5mN$ and specific impulse of $1200s$[21] and their profiles are reported in Figure 3 together with the evolution of the mean values of the orbital parameters changed during each maneuver.

Combined Maneuvers Strategy

A second maneuvering strategy is derived from literature[22] and enables to evaluate combined changes amongst the set of orbital parameters under the effect of the second-order zonal harmonics of the Earth's gravitational potential. Also in this case, analytical expressions to estimate the overall ΔV required to reach a desired target orbit are available, with the important remark that combined changes on the orbital parameters can be taken into account. Also in this case, the assumptions introduced in this subsection for true anomaly and RAAN phasing are applied.

In order to provide a better understanding of the differences between the two maneuvering strategies, the reference maneuver introduced in this subsection is considered and simulated with the same set of parameters. Results are shown in Figure 5, where a single transfer maneuver is employed to reach the desired target orbit.

PROBLEM FORMULATION

Optimization Problem

The reconfiguration problem is formulated as a multi-objective optimization with the goal of maximizing the observation performance over a given area of interest while minimizing the cost of the maneuvers needed to reach the target configuration. The initial constellation pattern is specified through the keplerian elements of its orbits and is taken as input for the optimization together with the payload FOV half-angle, the area of interest given in terms of latitude and longitude intervals and the desired number of orbital planes in the target configuration. The design variables and the constraints for the optimization are instead shown in Table 1, where $[a, e, i, \Omega, \omega, \nu]$ represents the set of keplerian parameters of the target configuration and N_P, N_S are respectively its number of orbital planes and satellites.

An important remark is that the admissible range for eccentricity values depends on the actual semi-major axis used during the optimization. In particular, proper lower and upper bounds e_{low}, e_{up}

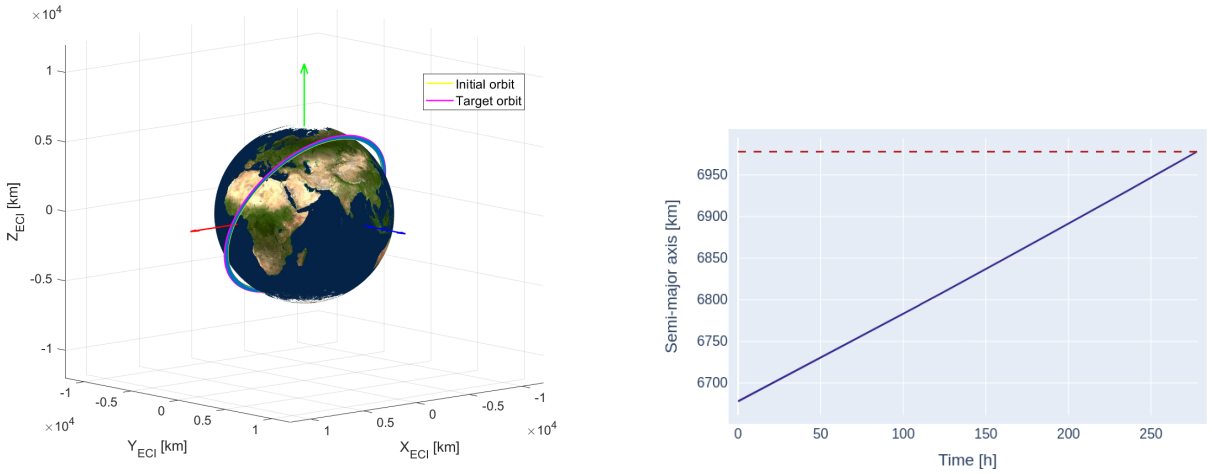

(a) Semi-major Axis Change Maneuver

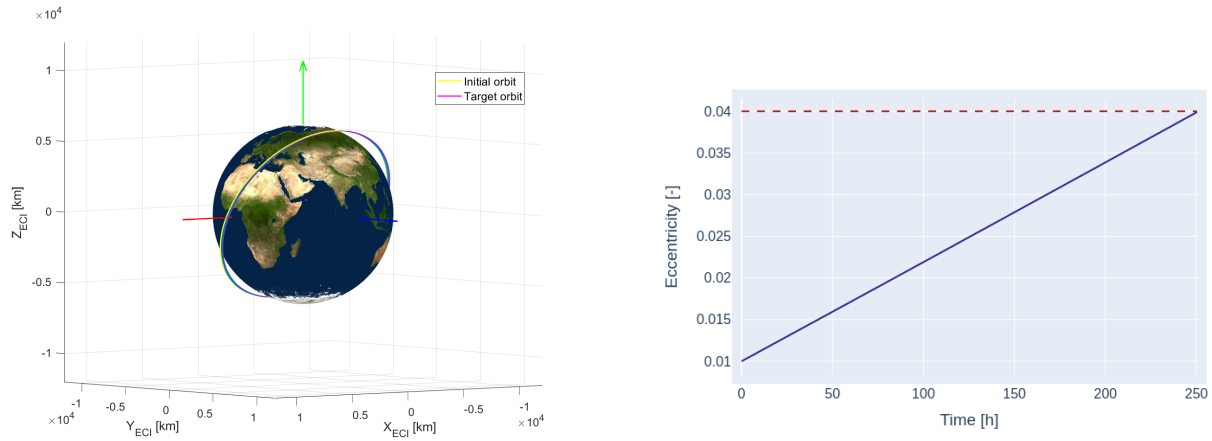

(b) Eccentricity Change Maneuver

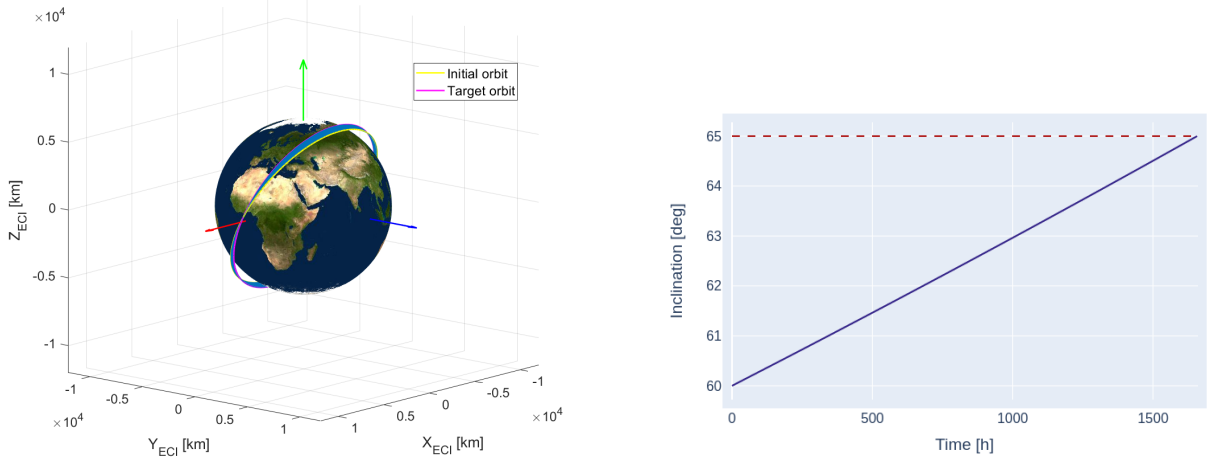

(c) Inclination Change Maneuver

Figure 3: Orbit Change with Separate Maneuvers Strategy

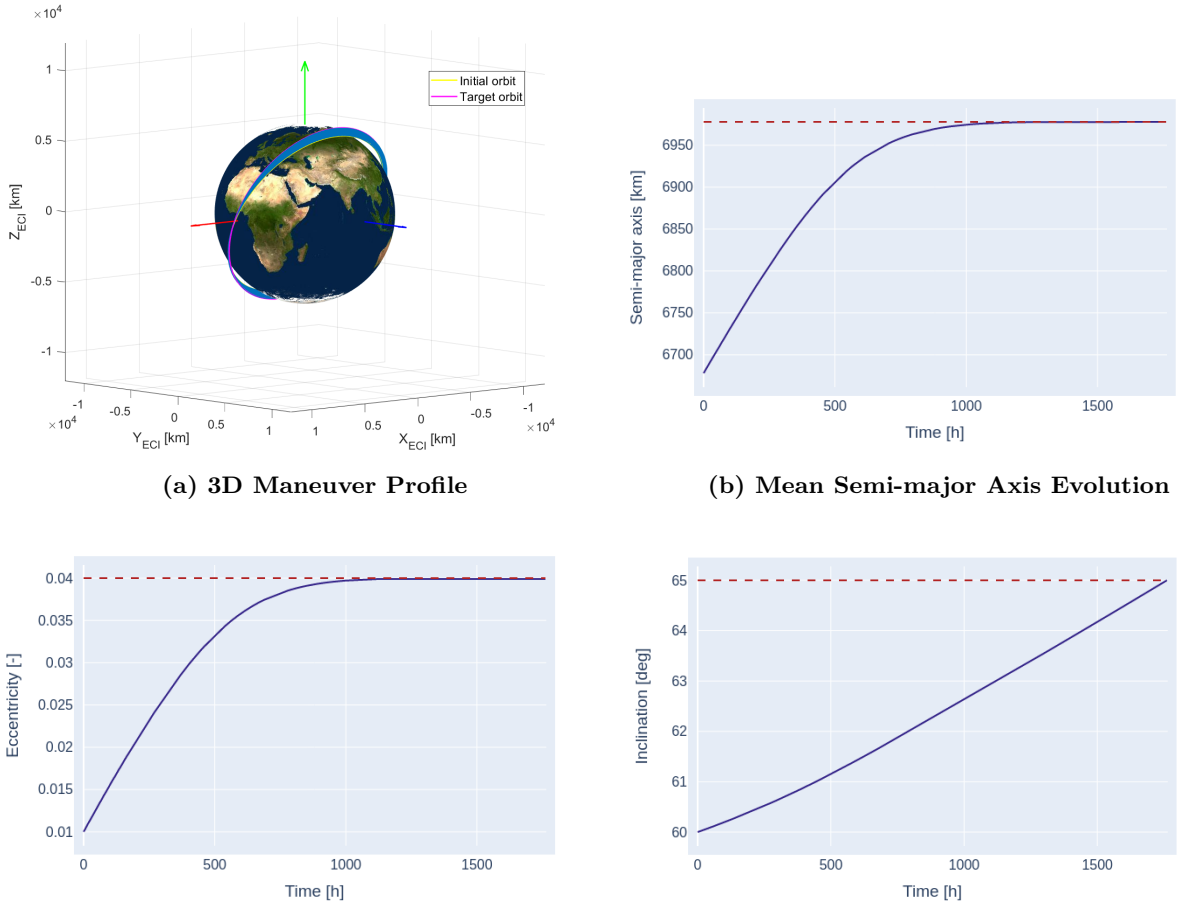

(a) 3D Maneuver Profile

(b) Mean Semi-major Axis Evolution

(c) Mean Eccentricity Evolution

(d) Mean Inclination Evolution

Figure 5: Orbit Change with Combined Maneuvers Strategy

should be enforced to guarantee the followings:

$$\begin{cases} r_p = a(1-e) \geq 6671km \\ r_a = a(1+e) \leq 7393km \end{cases} \tag{4}$$

where r_p, r_a are the radius at the periapsis and apoapsis.

Table 1: Design Variables in the Optimization

Variable	Number	Range
a	N_P	$6778 - 7178km$
e	N_P	$e_{low} - e_{up}$
i	N_P	$0 - 90\,\text{deg}$
Ω	N_P	$0 - 360\,\text{deg}$
ω	N_P	$0 - 360\,\text{deg}$
ν	N_S	$0 - 360\,\text{deg}$

Genetic Algorithm for Constellation Reconfiguration

Genetic Algorithms (GAs) are evolutionary stochastic search methods that mimic the mechanisms of natural evolution. They work on string-like structures that are evolved in time according to selection and reproduction processes aimed to preserve the fittest individuals. GAs have been applied to a wide range of optimization problems,[23] proving their effectiveness in dealing with nonlinear multi-parametric optimizations.[24] Also, their suitability to address orbit design and reconfiguration problems is already discussed in literature.[3,25]

GA-based optimization is chosen to deal with the complexity of the reconfiguration problem and guarantee a trade-off between a set of conflicting objectives. The overall optimization routine evolves towards optimal configurations starting from a population of randomly generated individuals by follow-

ing the iterative procedure represented in Figure 6.

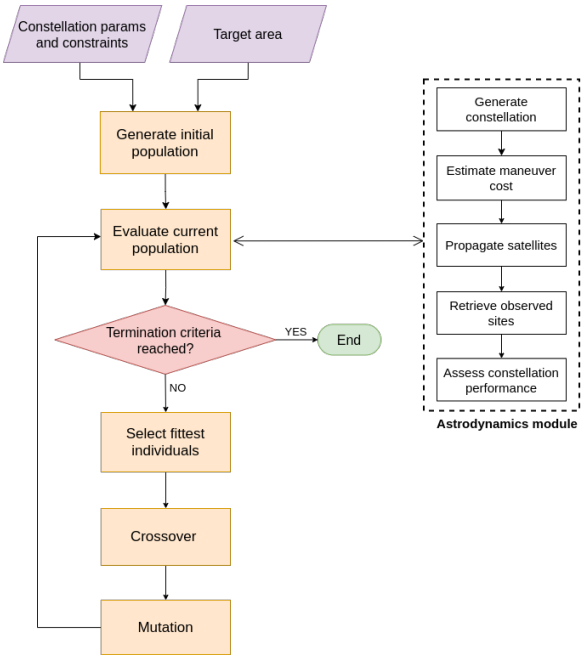

Figure 6: GA Evolution

The parameters of an individual are encoded in a structure called Chromosome, made up of an array of real values representing the orbital parameters. At each evolution step, candidate solutions are evaluated and ranked through a proper fitness function. As already discussed in this subsection, the evaluation process is implemented in a parallel fashion[26] by distributing among several processes the overall computational load to propagate the satellites in the constellation.

Once that the current population has been ranked, a new generation is built by relying on proper selection and reproduction mechanisms. In order to preserve the fittest individuals and prevent them from undergoing any modification, an elitism strategy is implemented.[27] The remaining spots in the generation are populated by selecting some individuals to mate and generate off-springs. Parent selection is crucial in determining the convergence rate of the GA, since good parents drive the evolution towards fitter solutions. However, good diversity should be maintained while generating new individuals to prevent an extremely fit solution to take over the entire population in few generations, causing premature convergence of the algorithm. In our work, a K-way tournament selection[28] is chosen amongst the methods available in literature.[29]

Starting from the selected parents, offsprings are generated from the parents' genetic inheritance (crossover). A simulated binary strategy is adopted[30] and an adaptive implementation[31] is chosen to decrease the maximum distance from the parents' values while the evolution is proceeding. Some genes inside the newly assembled children are randomly altered with a certain probability (mutation) to allow diversity in the population.

Evolution proceeds until some termination conditions computed from relevant population statistics are met. In particular, three main thresholds are considered to stop the optimization: a target fitness value, an upper limit on the number of generations and a lower limit in the best-fitness gradient across generations.

Fitness Function

The core of the optimization problem is represented by the fitness function, that should be defined so as to effectively synthesize the different optimization objectives. Both observation performance over the target area and maneuvering cost have to be taken into account to assign fitness scores and rank the current generation. A multi-objective optimization is therefore built up in the form of a minimization problem where the overall fitness function is expressed as:

$$J = \min_{x} \sum_{c=1}^{N_c} w_c f_c(x) \tag{5}$$

where the terms f_c represent the different objectives and w_c are the weights used to quantify the importance of the different contributions. It is important to notice that, in order to apply this weighted sum approach, the objective functions should be normalized so that their values are in similar magnitudes. In our case, the fitness contributions are normalized inside $[0; 1]$.

The optimization objectives are chosen to quantify the coverage and the revisit time factors of each configuration and the maneuvering cost. The percent coverage of the area of interest is used to measure the portion of the target area that is observed during the simulation, expressed as the number of points covered divided by the total number of points in the grid. However, the revisit time should also be included to provide information about the distribution of the observation gaps, defined as the length of time in which a point is not covered by any of the satellites in the constellation. The cost of the maneuvers needed to reach the final configuration is estimated as described in this subsection by assessing the required change in velocity ΔV.

The overall fitness function is therefore repre-

sented through the following five normalized contributions:

1. Maximum area percent coverage

$$f_1 = 1 - \frac{\sum_{i=1}^{N_i} coverage\ flag_i}{N_i} \tag{6}$$

2. Maximum area time coverage

$$f_2 = 1 - \frac{\sum_{i=1}^{N_i} \sum_{k=1}^{N_k} coverage_{ik}}{N_i N_k} \tag{7}$$

3. Maximum area revisit time

$$f_3 = \frac{\sum_{i=1}^{N_i} max\ revisit_i}{N_i N_k} \tag{8}$$

4. Average area revisit time

$$f_4 = \frac{\sum_{i=1}^{N_i} revisit_i}{N_i N_k} \tag{9}$$

5. Maneuver cost

$$f_5 = \sum_{s=1}^{N_s} \frac{\Delta V_s}{\Delta V_s^{max}} \tag{10}$$

where subscripts i, k, s represent respectively a specific site, time step and satellite while N_i, N_k, N_s are the overall number of target sites, propagation steps and satellites in the constellation. The $coverage\ flag_i$ indicates if a specific target point i in the area of interest is observed along the propagation horizon while $coverage_{ik}$ is a boolean value to express if the target i is accessed at time instant k.

The maximum available change in velocity for each satellite ΔV_s^{max} can be derived from mission requirements and it is used as a normalization term for the maneuver cost contribution.

Maneuvers Cost Estimation

As described before, the orbital low-thrust maneuvers implying single parameters modifications are retained from literature.[18]
In this chapter an overview of the costs for LEO orbit changes is given by estimating the required ΔV in case of the orbital transfer described in Table 2. The initial configuration is a Walker-δ (64)6/3/2 that will be considered also later in this section as the starting constellation for the reconfiguration maneuvers.

The contour plots in Figure 8 display the costs for single parameters change maneuvers in the simple case reported in Table 2. It is easy to notice that in this case the most demanding maneuver is represented by the change of inclination, as displayed in figures. Since the purpose of this chapter is to quantify the costs for LEO orbit changes, the four maneuvers are assumed to be performed separately and they are computed starting from the reference Walker configuration.

Table 2: Reference Walker 6/3/2

Parameter	Unit	Initial value	Target value
a	km	6978	7078
e	[-]	0.01	0.02
i	deg	64	60
ω	deg	10	50

In Figure 7a, 7b, 7c the initial values of a, e, i are plotted against the target ones. The estimated cost for the desired changes on these parameters is therefore represented by the ΔV band in which the grey point is located. In Figure 7d the argument of the perigee is instead plotted with respect to the eccentricity and the maneuver is represented as the requested variation of ω at the given e.

SIMULATION RESULTS

Simulation Scenario

The proposed reconfiguration strategy is tested in a LEO environment, considering a desired change in the observation requirements from a global coverage mode to a regional one. Two different scenarios are analyzed to investigate GA-based reconfiguration performance in case specific targets or regional observations are requested.

A constellation of six satellites equally distributed in three orbital planes is considered. Imaging sensors with an half-angle of 10 deg are assumed to show the advantages of reconfiguration in limited coverage scenarios. The initial constellation is designed as a Walker-δ (64)6/3/2,[32] chosen to represent the global coverage mode.

Simulations are carried out starting from May 1^{st}, 2021. A horizon of 48 hours is used in the narrow region of interest scenario, while an overall duration of 24 hours is employed in case of a wider ROI; the time step is instead fixed to 60 sec. An important remark is that this time step value only refers to GA optimization, that highly benefits from lower computational loads. However, performance analysis reported in this subsection are executed with a time step of 10 sec. As already highlighted in this subsection, a multi-processing architecture is employed to

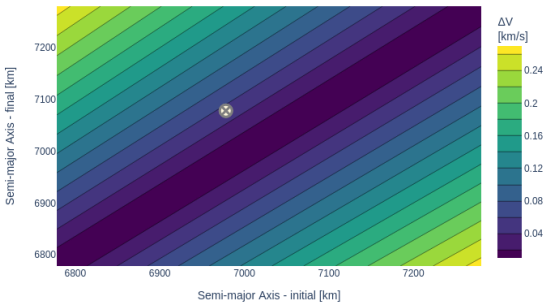

(a) Semi-major Axis Change Maneuver

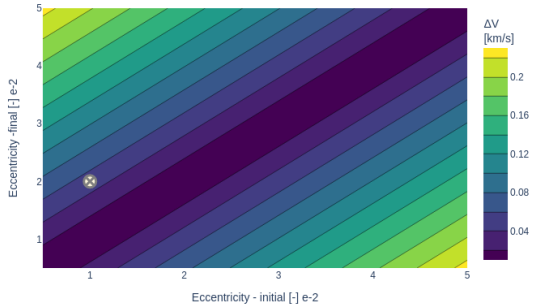

(b) Eccentricity Change Maneuver

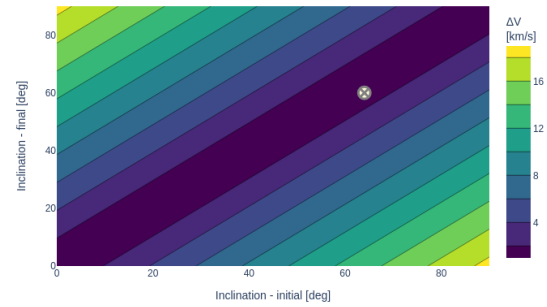

(c) Inclination Change Maneuver

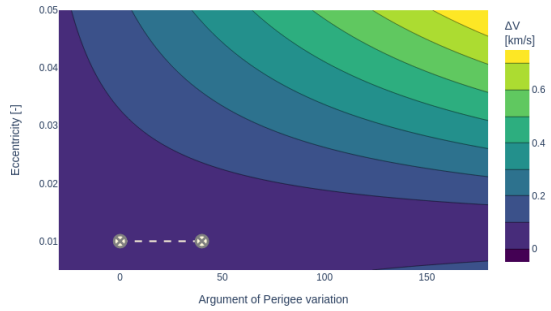

(d) Argument of Perigee Change Maneuver

Figure 8: Single Maneuvers Costs for the Orbital Transfer Reported in Table 2

speed-up the evaluation process. In particular, we adopt six different processes, one for each satellite in the constellation.

Repeating Ground Track Orbits

Repeating ground track orbits (RGT) are commonly used for regional or specific target observations as they offer enhanced partial coverage properties while being easy to design.[3] Moreover, a RGT constellation can be reached by simply adjusting its satellites' altitudes so as to obtain the desired RGT ratio τ. In particular, considering a satellite that orbits around Earth exactly N_P times in N_D days, its RGT ratio can be expressed as described in literature:[15]

$$\tau = \frac{N_P}{N_D} = \frac{n + \Delta n + \dot{\omega}}{\omega_E - \dot{\Omega}} \tag{11}$$

where n is the mean motion of the satellite, $\dot{M} = n + \Delta n$ is the perturbed mean motion, ω_E is the rotation rate of the Earth, $\dot{\omega}$ is the drift rate of the argument of the perigee due to perturbations and $\dot{\Omega}$ is the nodal regression rate due to perturbations.

RGT orbits are therefore studied together with the GA-based optimization to analyze if more freedom during the optimization phase could lead to comparable observation performance over the target sites while requiring a smaller change in velocity. In particular, proper constraints derived from equation 11 are implemented inside the GA to force the final solution to assume a RGT pattern. When the constraint is active, the orbits of the target configuration are characterized by an integer RGT ratio τ and belong to one of the curves shown in Figure 11a, where the relationship between the semi-major axis and the inclination are reported for sample RGT ratios. The effect of eccentricity in RGT orbits design is depicted in Figure 11b and demonstrates how,

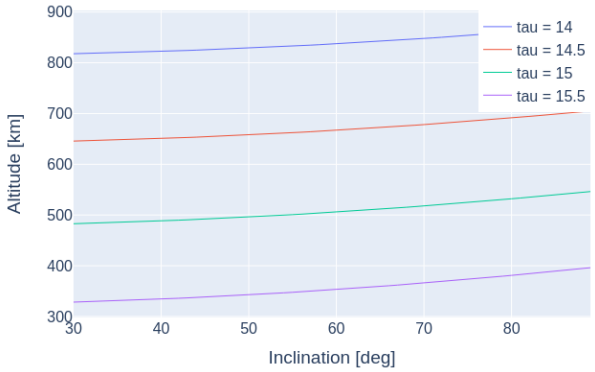

(a) RGT Altitude as a Function of Inclinations and Frequencies

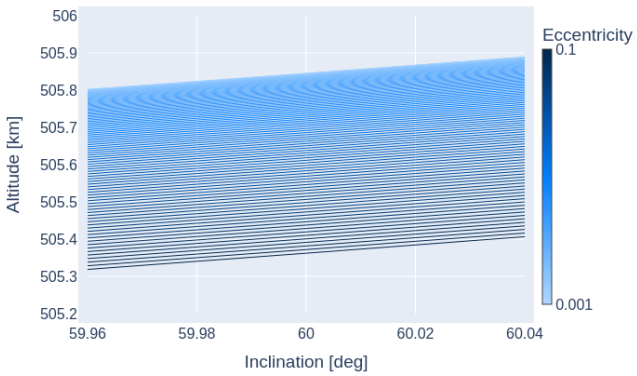

(b) RGT Altitude as a Function of Eccentricities with a Fixed Frequency of 15

Figure 10: Repeating Ground Track Orbits at Different Inclinations and Frequencies

considering a fixed inclination, the RGT semi-major axis undergoes a small increase with the eccentricity. Values up to $e = 0.1$ are shown as this work is focused on LEO orbits according to the boundaries reported in Table 1.

Narrow ROI Scenario

The tests reported in Table 3 are carried out to analyze the GA performance in a scenario in which the observation of a narrow area located between latitudes $48 - 49$ deg and longitudes $5 - 6$ deg is requested. The arranged test cases are devised so as to study the results produced by the optimization in scenarios with an increasing number of optimization variables. Also, RGT constraints are included in the problem as described in this subsection to enforce a Repeating Ground Track pattern in the final constellation configuration. All the runtimes refer to the execution on a workstation equipped with an 8-core, 4.2GHz AMD Threadripper 2990WX CPU and 16GB of RAM.

Numerical results for the defined test cases are reported in Table 4, where the best results for the different objectives are collected and the improvement with respect to the performance achievable in the global coverage mode with the Walker-δ pattern is shown. The first objective representing the percent coverage of the region of interest is not reported as the target is always accessed at least one time during the overall horizon. The other metrics corresponding to maximum time coverage, maximum revisit time, average revisit time of the target and average maneuvering cost for each satellite in the constellation are instead displayed.

Table 4: Obtained Objectives in the Narrow ROI Scenario

Test case	f2 [min]	f3 [h]	f4 [h]	f5 [m/s]
Walker-δ	1	31.93	23.99	-
0	14	7.866	3.18	48.117
1	7.2	7.95	5.87	2.708
2	9.3	8.1	4.68	6.667
3	14	7.88	3.18	195
4	11	7.73	3.98	169
5	10	7.9	4.07	253
6	10.98	7.93	3.98	49
7	12.6	7.85	3.54	312
8	16	6.76	2.8	700

By analyzing the results in Table 4, it is possible to conclude that the RGT pattern seems a suitable choice to reconfigure the constellation for a single-target observation. Savings in the requested ΔV can be obtained by giving more freedom to the optimization process. In this way, reduced costs are achieved in exchange for a slight worsening in the observation performance. Also, enhanced coverage and revisit time could be achieved by increasing the cost of the maneuver. The optimized configurations coming from Test 0 and Test 2 as defined in Table 3 are shown in Figure 12. By looking at the coverage geometry of the two constellations, the validity of a RGT pattern to observe a narrow region is confirmed. However, in case of multiple targets, the RGT solution shows its limits, especially if payloads have very small FOV with coverage not far from the linear ground track path. In these situations a more unconstrained solution could reveal its advantages.

Table 3: Test Cases in the Narrow ROI Scenario

Test case	RGT	Maneuvering	Optimization variable						GA parameters			Runtime
			a	e	i	Ω	ω	ν	Pop size	Max gen	Elitism	
0	Yes	Separate	1					6	100	100	5	747 min
1		Separate	1					6	100	100	5	752 min
2		Separate	3					6	120	100	6	798 min
3	Yes	Separate	1	3			3	6	150	100	8	927 min
4		Separate	3	3			3	6	150	100	8	983 min
5		Separate	3	3	3		3	6	150	150	8	1132 min
6		Combined	3	3			3	6	150	100	8	986 min
7		Combined	3	3	3		3	6	150	150	8	1160 min
8		Combined	3	3	3	3	3	6	150	150	8	1232 min

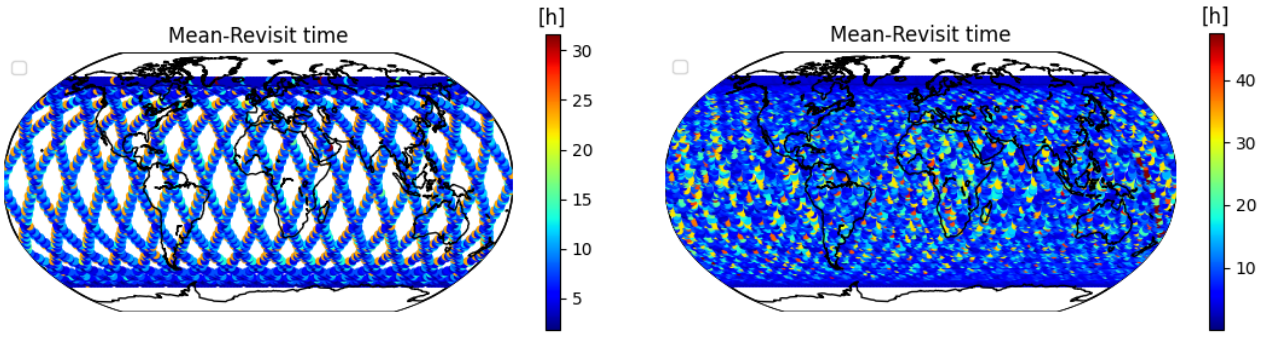

(a) Test Case 0 (RGT) **(b) Test Case 2 (non RGT)**

Figure 12: Mean Revisit Time for a Propagation Horizon of 24 Hours

Wide ROI Scenario

A second batch of tests is performed to analyze the GA performance in addressing reconfiguration problems when a wider region of interest is specified. This could be relevant when regional coverage over a certain area should be enforced or when multiple targets are distributed across a shared portion of the Earth surface. The desired region of interest is specified in terms of latitude-longitude intervals and the corresponding subsection of the Earth grid retrieved as described in this section is used to identify the target points. The simulations reported in this subsection take as input an area located in central Europe between latitudes $40-65$ deg and longitudes $5-17$ deg.

Two different solutions coming from the GA-based approach are compared in this section: at first a RGT pattern is produced by enforcing the proper constraints on the semi-major axis of the target constellation, then the whole set of orbital parameters is freely optimized considering a maximum ΔV for each satellite equal to $500 m/s$. The GA parameters are set to the following values: 200 max generations, a population size of 250 and an elitism equal to 8. The behavior of the overall fitness score is shown in Figure 14 together with the evolution of the normalized fitness scores (as defined in this subsection). The trends are aligned with the minimization objective, exhibiting a progression towards lower scores while maintaining a trade-off amongst the different contributions. These results are obtained by averaging the execution of several optimization runs with the same set of parameters so as to extract the mean trends of the GA and polish them from random fluctuations.

The obtained constellation configurations are reported in Table 5 by listing the optimized orbital parameters for the six satellites, where ν_1 represents the true anomaly of the first satellite in each orbital plane and θ is the in-plane phasing. The red color is used to indicate that RGT constraints are active.

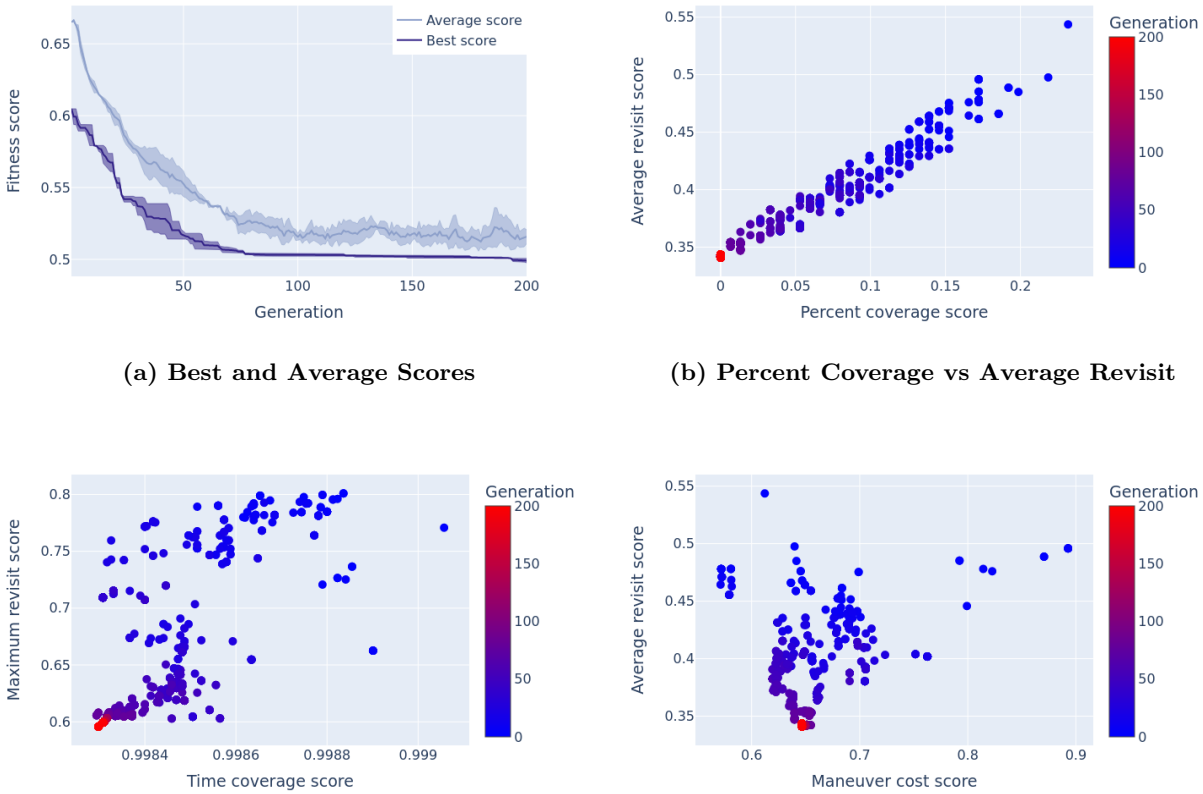

(a) Best and Average Scores

(b) Percent Coverage vs Average Revisit

(c) Time Coverage vs Maximum Revisit

(d) Maneuver Cost vs Average Revisit

Figure 14: Overall Fitness and Scores Evolution during GA Optimization

Table 5: GA-based Configurations

Variable	Unit	Plane #1	Plane #2	Plane #3
a	km	6890	6890	6890
		7046	7168	7157
e	–	0.01	0.01	0.01
		0.0005	0.0188	0.0295
i	deg	64	64	64
		63	64	64
Ω	deg	0	120	240
		107	73	234
ω	deg	0	0	0
		193	249	232
ν_1	deg	4	176	103
		201	91	52
θ	deg	21	145	122
		32	143	116

The average maneuvering cost of each satellite to reach the final configuration starting from the Walker-δ (64)6/3/2 is $20m/s$ and $110m/s$ respectively for the RGT and GA-based configuration.

The groundtracks of the two optimized configurations are shown in Figure 16 considering a single orbital period. It is possible to notice that when the whole set of orbital parameters are optimized, the GA places the three orbital planes at different inclinations, enabling a better coverage in the lower part of the region of interest.

The revisit time performance of the two configurations is analyzed in the following part of this section. In Figure 18 the average revisit time obtained in both cases is shown. A more accurate analysis is instead presented in Figure 20 and Figure 22, where the mean revisit time, maximum revisit time, minimum revisit time and average number of passes are reported for the whole Earth surface and the region of interest. All these figures are obtained considering

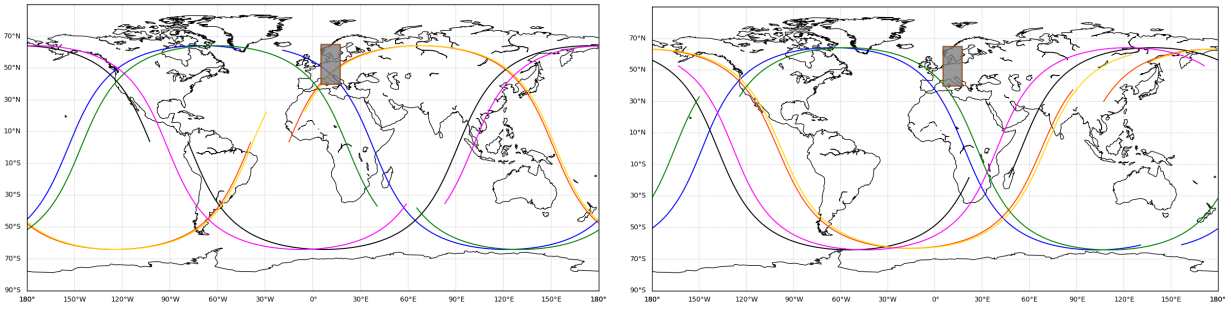

(a) GT of the RGT Configuration **(b) GT of the GA-based Configuration**

Figure 16: GT for a Single Orbital Period

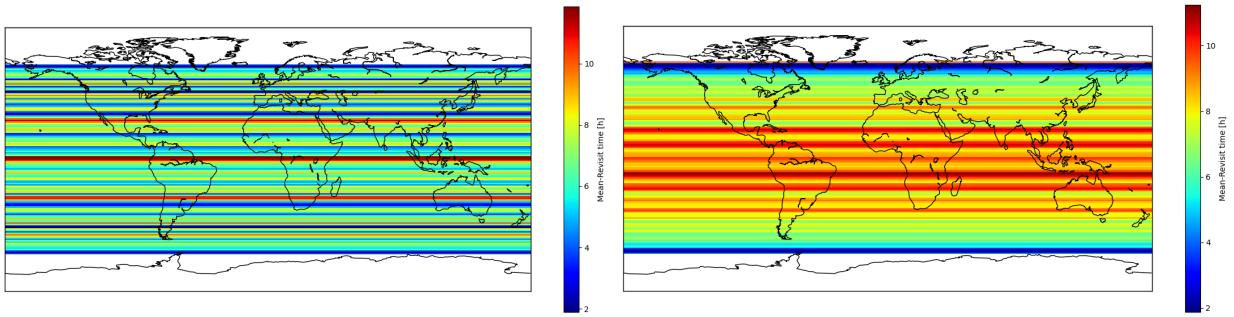

(a) Average Revisit of the RGT Configuration **(b) Average Revisit of the GA-based Configuration**

Figure 18: Average Revisit Time for a 24-hours Propagation Horizon

a 24-hours propagation horizon.

CONCLUSIONS AND NEXT STEPS

In this paper we propose a framework to analyze and evaluate low-thrust reconfiguration opportunities. A strategy to assess the benefits of reconfigurable constellations is developed and the enhanced observation performance over a given area of interest is compared to the cost needed to reach the target configuration. The reconfiguration problem is formulated as a multi-objective optimization in which a trade-off between access to the region of interest and cost of the maneuvers is produced. The goodness of the produced solutions in terms of observation performance is assessed through different figure of merits, including percent area coverage, average area coverage time, average revisit time and maximum revisit time. A Genetic Algorithm is exploited to carry out the optimization process, enabling to dynamically weight the different contributions to the fitness function in accordance to the user needs.

A reconfiguration from a global coverage mode, represented by a Walker-δ pattern, and a regional coverage mode is investigated. A LEO constellation composed of six satellites distributed in three orbital planes is used to demonstrate the developed algorithm and a combination of $a, e, i, \Omega, \omega, \nu$ are chosen as optimization variables. Several test cases are defined to study the behavior of the optimization routine considering an increasing number of free orbital parameters. A Repeating Ground Track configuration is also analyzed against the results produced by the GA in terms of observation performance and reconfiguration cost.

Relying on the results presented in this paper, future work will be done to make the problem closer to a real scenario so as to test the presented strategy for possible applications.

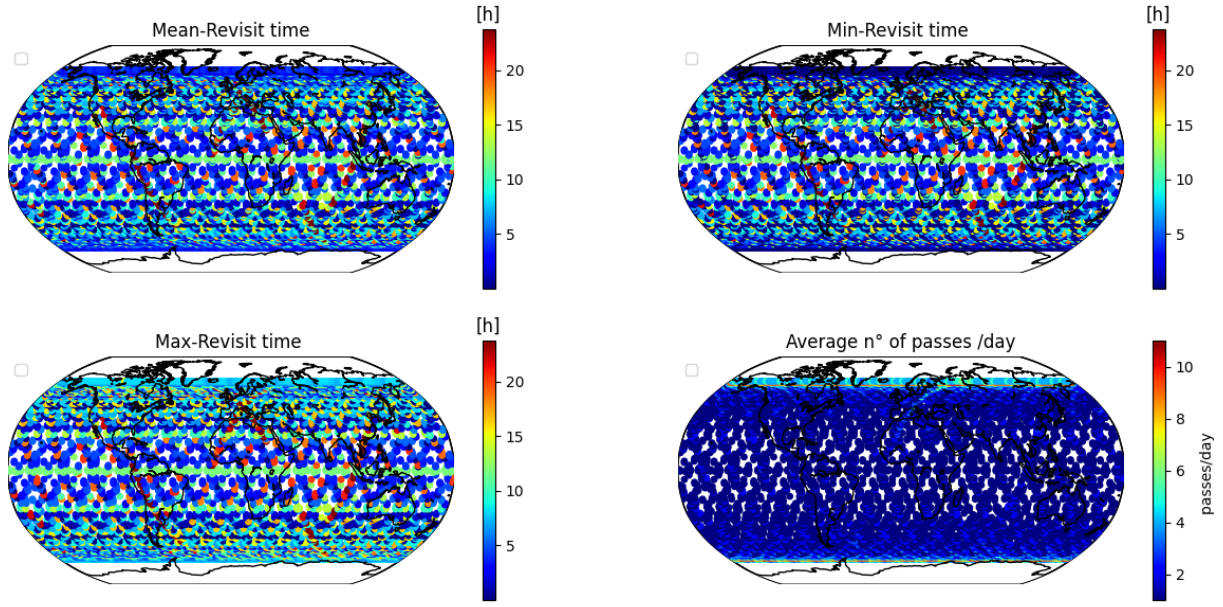

(a) Global Performance Metrics of the RGT Configuration

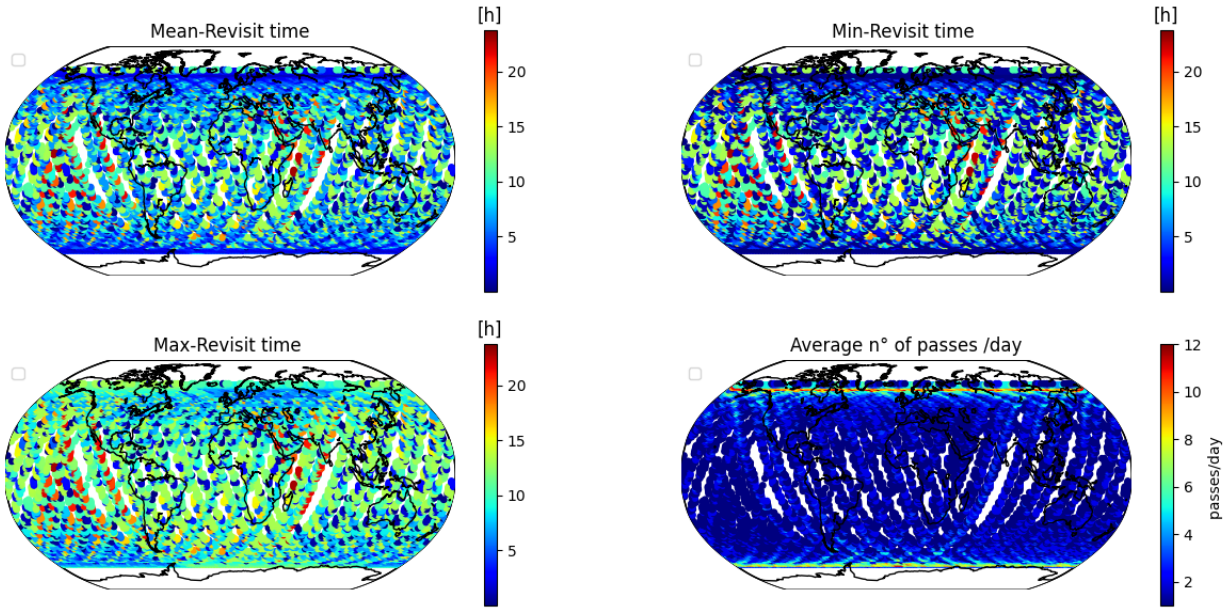

(b) Global Performance Metrics of the GA-based Configuration

Figure 20: Global Performance Metrics for a 24-hours Propagation Horizon

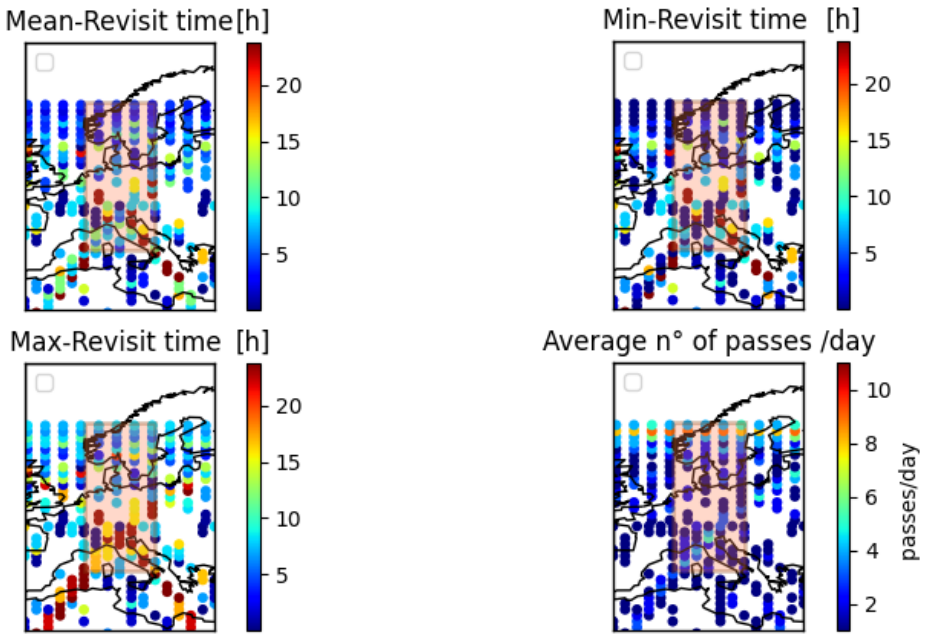

(a) Local Performance Metrics of the RGT Configuration

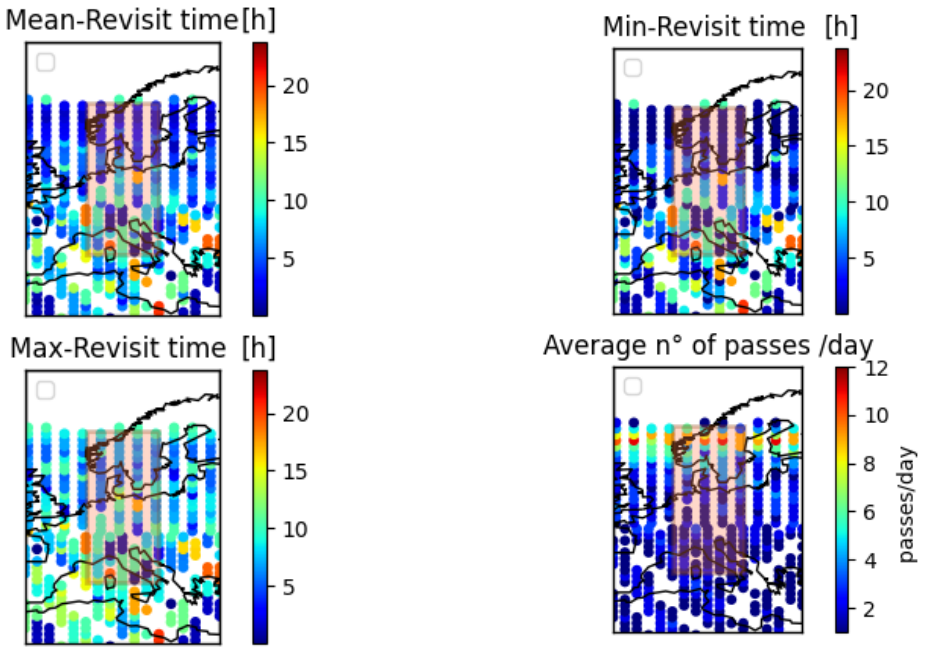

(b) Local Performance Metrics of the GA-based Configuration

Figure 22: Local Performance Metrics for a 24-hours Propagation Horizon

References

[1] Shuang Zhao, Yanli Xu, and Huayu Dai. Research on the configuration design method of heterogeneous constellation reconstruction under the multiple objective and multiple constraint. *AIP Conference Proceedings*, 1839(1):020083, 2017.

[2] Michael Hlas and Jeremy Straub. An autonomous satellite debris avoidance system. In *2016 IEEE Aerospace Conference*, pages 1–5, 2016.

[3] Sung Wook Paek, Sangtae Kim, and Olivier de Weck. Optimization of reconfigurable satellite constellations using simulated annealing and genetic algorithm. *Sensors*, 19(4), 2019.

[4] Aerospace Corporation. Constellation reconfiguration, 2019. .

[5] Afreen Siddiqi. *Reconfigurability in space systems : architecting framework and case studies*. PhD thesis, Massachussets Institute of Technology, 2006.

[6] Uriel Scialom. *Optimization of satellite constellation reconfiguration*. PhD thesis, Massachusetts Institute of Technology, 2003.

[7] J.J. Davis. *Constellation Reconfiguration: Tools and Analysis*. PhD thesis, Texas A & M University, 2011.

[8] Matthew P. Ferringer, D. Spencer, and P. Reed. Many-objective reconfiguration of operational satellite constellations with the large-cluster epsilon non-dominated sorting genetic algorithm-ii. *2009 IEEE Congress on Evolutionary Computation*, pages 340–349, 2009.

[9] S.W. Paek. Reconfigurable satellite constellations for geo-spatially adaptive earth observation missions. Master's thesis, Massachussets Institute of Technology, 2012.

[10] Wiley J. Larson and James Richard Wertz. *Space mission analysis and design*. Microcosm, 1992.

[11] Patrick W Kenneally, Scott Piggott, and Hanspeter Schaub. Basilisk: a flexible, scalable and modular astrodynamics simulation framework. *Journal of aerospace information systems*, 17(9):496–507, 2020.

[12] Byron Tapley, J.C. Ries, Srinivas Bettadpur, D. Chambers, Molin Cheng, F. Condi, and S. Poole. The ggm03 mean earth gravity model from grace. *AGU Fall Meeting Abstracts*, -1:03, 11 2007.

[13] David A Vallado. *Fundamentals of astrodynamics and applications*, volume 12. Springer Science & Business Media, 2001.

[14] Michel Raynal. Concurrent programming: Algorithms, principles, and foundations. In *Springer Berlin Heidelberg*, 2013.

[15] Michel Capderou. *Handbook of Satellite Orbits*. 01 2014.

[16] Z. Malkin. On subdivision of spherical surface into equal-area cells. *arXiv: Instrumentation and Methods for Astrophysics*, 2016.

[17] Ciara McGrath and Malcolm Macdonald. Design of a reconfigurable satellite constellation. In *66th International Astronautical Congress, IAC2015*, pages Paper–IAC, 2015.

[18] Armando Ruggiero, Pierpaolo Pergola, Salvo Marcuccio, and Mariano Andrenucci. Low-thrust maneuvers for the efficient correction of orbital elements. In *32nd International Electric Propulsion Conference*, pages 11–15, 2011.

[19] Roger R. Bate, Donald D. Mueller, and Jerry E. White. *Fundamentals of Astrodynamics*. Dover Publications, New York, 1971.

[20] Olivier Zarrouati. *Trajectoires spatiales*. 1987.

[21] Paul Lascombes. Electric propulsion for small satellites orbit control and deorbiting: The example of a hall effect thruster. In *2018 SpaceOps Conference*, page 2729, 2018.

[22] Marilena Di Carlo and Massimiliano Vasile. Analytical solutions for low-thrust orbit transfers. *Celestial Mechanics and Dynamical Astronomy*, 133(7):1–38, 2021.

[23] Oliver Kramer. *Genetic Algorithms*. Springer International Publishing, Cham, 2017.

[24] David E. Goldberg. *Genetic Algorithms in Search, Optimization and Machine Learning*. Addison-Wesley Longman Publishing Co., Inc., USA, 1st edition, 1989.

[25] Xiangyue He, Haiyang Li, Luyi Yang, and Jian Zhao. Reconfigurable satellite constellation design for disaster monitoring using physical programming. *International Journal of Aerospace Engineering*, 2020:1–15, 2020.

[26] Erick Cantú-Paz et al. A survey of parallel genetic algorithms. *Calculateurs paralleles, reseaux et systems repartis*, 10(2):141–171, 1998.

[27] Robin C Purshouse and Peter J Fleming. Why use elitism and sharing in a multi-objective genetic algorithm? In *Proceedings of the 4th Annual Conference on Genetic and Evolutionary computation*, pages 520–527, 2002.

[28] Yongsheng Fang and Jun li. A review of tournament selection in genetic programming. pages 181–192, 10 2010.

[29] Noraini Razali and John Geraghty. Genetic algorithm performance with different selection strategies in solving tsp. volume 2, 01 2011.

[30] Kalyanmoy Deb, Ram Bhushan Agrawal, et al. Simulated binary crossover for continuous search space. *Complex systems*, 9(2):115–148, 1995.

[31] Kalyanmoy Deb, Karthik Sindhya, and Tatsuya Okabe. Self-adaptive simulated binary crossover for real-parameter optimization. In *Proceedings of the 9th Annual Conference on Genetic and Evolutionary Computation*, GECCO '07, page 1187–1194, New York, NY, USA, 2007. Association for Computing Machinery.

[32] John G Walker. Satellite constellations. *Journal of the British Interplanetary Society*, 37:559, 1984.